Geophysical Research Letters

RESEARCH LETTER
10.1029/2025GL116050

Large Surface-Rupturing Earthquakes and a >12 kyr, Open Interseismic Interval on the Tintina Fault, Yukon

Theron Finley[1], **Edwin Nissen**[1,2], **John F. Cassidy**[1,3], **Guy Salomon**[1], **Lucinda J. Leonard**[1], **and Duane Froese**[4]

[1]School of Earth and Ocean Sciences, University of Victoria, Victoria, BC, Canada, [2]College of Earth, Atmospheric, and Ocean Sciences, Oregon State University, Corvallis, OR, USA, [3]Pacific Geoscience Centre, Geological Survey of Canada, Natural Resources Canada, Sidney, BC, Canada, [4]Department of Earth and Atmospheric Sciences, University of Alberta, Edmonton, AB, Canada

Key Points:

- We provide the first conclusive evidence of numerous large (>M_w 7.5) surface-rupturing earthquakes in the Quaternary on the Tintina fault
- Offsets to Early and Middle Pleistocene glaciofluvial terraces and moraines indicate a slow dextral slip rate of 0.2–0.8 mm/yr
- Late Pleistocene terraces are undeformed across the fault, indicating >12 kyr have elapsed since the most recent earthquake

Supporting Information:

Supporting Information may be found in the online version of this article.

Correspondence to:

T. Finley,
tfinley@uvic.ca

Citation:

Finley, T., Nissen, E., Cassidy, J. F., Salomon, G., Leonard, L. J., & Froese, D. (2025). Large surface-rupturing earthquakes and a >12 kyr, open interseismic interval on the Tintina fault, Yukon. *Geophysical Research Letters*, *52*, e2025GL116050. https://doi.org/10.1029/2025GL116050

Received 20 MAR 2025
Accepted 17 JUN 2025

Author Contributions:

Conceptualization: Theron Finley
Data curation: Theron Finley
Formal analysis: Theron Finley
Funding acquisition: Theron Finley, Edwin Nissen, John F. Cassidy
Investigation: Theron Finley, Guy Salomon
Methodology: Theron Finley, Edwin Nissen, John F. Cassidy, Guy Salomon
Project administration: Theron Finley, Edwin Nissen, John F. Cassidy

Abstract We present the first geomorphic evidence for successive, surface-rupturing earthquakes throughout the Quaternary on the Tintina fault in the Yukon Territory, northwestern Canada. A ~130-km-long series of scarps and pressure ridges offset 2.6 Ma and 132 ka landforms by ~500–1,500 m and 65–85 m, respectively, indicating a dextral slip rate of ~0.2–0.8 mm/yr. However, early Holocene terraces are undeformed across the fault, implying that the elapsed time since the most recent earthquake is >12 kyr and that the fault may be nearing the end of a long interseismic cycle. A minimum slip deficit of ~6 m has likely accrued since the last major surface rupture, and future earthquakes could exceed M_w 7.5. These results highlight the hazards of earthquakes on mature, low-slip-rate intraplate faults, which may have exceptionally long recurrence intervals, elude instrumental networks, and lack a distinct surface expression due to landscape resetting.

Plain Language Summary The Tintina fault is a major ~1,000-km-long geologic fault in the Yukon Territory of northwestern Canada, previously believed to have last been active around 40 million years ago, but speculated to remain capable of generating large earthquakes. Using new high-resolution topographic data collected from satellites, airplanes, and drones, we have identified a 130-km-long segment of the fault where 2.6 million-year-old, and 132 thousand-year-old geological formations are laterally shifted across the fault by ~1,000 and 75 m, respectively. From this, we surmise that the Tintina fault has ruptured in numerous large earthquakes in the recent geologic past, and continues to accumulate strain at an average rate of 0.2–0.8 mm/yr. We further show that the fault has not ruptured in a major earthquake for at least 12 thousand years, and could generate an earthquake of at least magnitude 7.5 in the future. The Tintina fault therefore represents an important, previously unrecognized, seismic hazard to the region.

1. Introduction

Identifying and characterizing seismogenic faults in slowly deforming regions is a major challenge for seismic hazard analysis. Microseismicity often does not align (or even exist) along such faults, geodetic networks commonly lack the precision to resolve sub-millimeter/year slip rates, and low-strain-rate regions are generally a low priority for dense instrumentation. Recurrence intervals between large earthquakes on low-slip-rate faults can be both long and irregular (Bollinger et al., 2021; Griffin et al., 2020; Nicol et al., 2016; Yuan et al., 2018), and consequently, multi-event paleoseismic and tectono-geomorphic records are rare. This issue is exacerbated in young landscapes reset by icesheets or other climatic factors, where faults have not had time to accrue significant offset of the youngest surfaces. Seismic hazard models in these regions typically rely on area sources based on historical seismicity alone, which may not capture the maximum credible earthquake or the potential for surface rupture. Notably, low-slip-rate faults are shown to produce larger magnitude earthquakes with greater static stress drops than faster slipping faults with comparable rupture lengths, underscoring the importance of characterizing them (Anderson et al., 2017).

In this paper we examine the Tintina fault, a major, structurally mature fault, that occupies a pronounced, northwest-trending, ~1,000-km-long valley known as the Tintina Trench in the Yukon Territory, northwestern Canada (Figure 1; Gabrielse et al., 2006). It connects NW to the Kaltag fault in Alaska, and SE to the Rocky Mountain Trench fault in British Columbia. The Tintina fault is shown to have accrued ~430 km of cumulative dextral offset, largely in the Eocene (Gabrielse et al., 2006), and may have slipped at rates as high as 13 mm/yr (Ryan et al., 2017), making it an end member in terms of structural maturity. However, its activity has since

Resources: Theron Finley, Edwin Nissen, John F. Cassidy
Supervision: Edwin Nissen, John F. Cassidy
Validation: Edwin Nissen, John F. Cassidy, Guy Salomon, Lucinda J. Leonard, Duane Froese
Visualization: Theron Finley
Writing – original draft: Theron Finley
Writing – review & editing: Theron Finley, Edwin Nissen, John F. Cassidy, Guy Salomon, Lucinda J. Leonard, Duane Froese

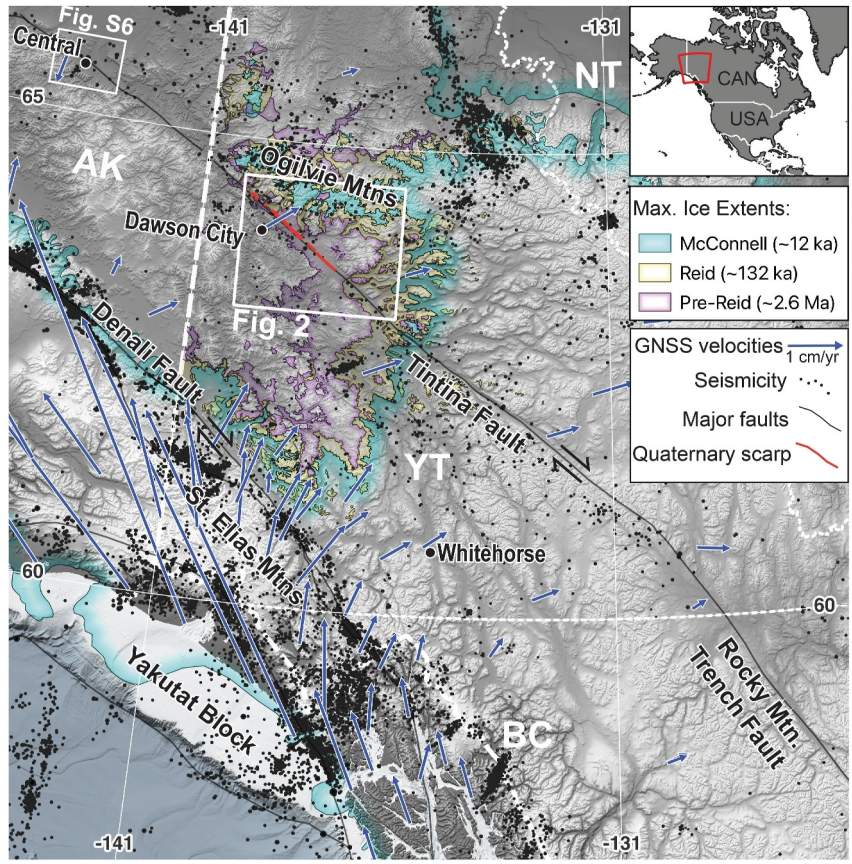

Figure 1. Physiography and seismotectonics of the Yukon Territory. Quaternary scarps along the Tintina fault in this study are highlighted with a red line. Maximum ice limits for the McConnell, Reid and Pre-Reid glaciations are from Dalton et al. (2023) and Duk-Rodkin (1999). Reid and Pre-Reid limits are not mapped beyond the Yukon Territory. Seismicity (Natural Resources Canada, 2024) and a subset of GNSS velocities relative to stable North America (Elliott & Freymueller, 2020) demonstrate a slow rate of deformation in the Cordilleran interior.

waned. There are low levels of diffuse seismicity along it (Drooff & Freymueller, 2023) with only ~2 earthquakes $\geq M_w$ 3.0 per year (Figure 1). Summing the seismic moment yields a slip rate of 0.5 (+0.9/−0.3) mm/yr, and geodetic block models struggle to resolve any slip (Elliott & Freymueller, 2020; Leonard et al., 2007, 2008). Strain from the ongoing Yakutat collision in southeast Alaska is transmitted across the entire northern Cordillera (Mazzotti & Hyndman, 2002; Figure 1), leading to suggestions that the Tintina fault may still be capable of large surface-rupturing earthquakes (Duk-Rodkin et al., 2001; Mortensen & Von Gaza, 1992). However, while Canada's National Seismic Hazard Model includes the potential for earthquakes up to M_w 7.8 in a broad ($>3 \times 10^5$ km^2) source area covering central Yukon Territory, the Tintina fault is not currently recognized as a discrete seismogenic fault source (Adams et al., 2019; Kolaj et al., 2023).

The landscape in northwestern Yukon is among the oldest in Canada, with high potential for preservation of tectonic landforms. Aside from a few isolated ice fields in the Ogilvie Mountains, much of the region remained ice-free during the most recent Late Pleistocene (late Wisconsinan), Marine Isotope Stage (MIS) 2 glaciation, locally referred to as the McConnell glaciation, which otherwise covered most of the Canadian Cordillera (Figure 1) between ~24 and 12 ka (Dalton et al., 2023; Stroeven et al., 2010). Several older and more spatially extensive glaciations did advance into northwestern Yukon (Duk-Rodkin, 1999): these are the late-Middle Pleistocene Reid glaciation (MIS 6), which ended at ~130 ka (Demuro et al., 2012), and several Late Pliocene-Middle Pleistocene Pre-Reid glaciations (0.2–2.6 Ma; Hidy et al., 2013). Sedimentation at the margins of these icesheets left moraines and glaciofluvial deposits with distinctive soils on their surfaces (Smith et al., 1986; Tarnocai et al., 1985) that, together with the absolute ages, provide constraint on the slip rate and timing of ruptures on the Tintina fault (Figure 2).

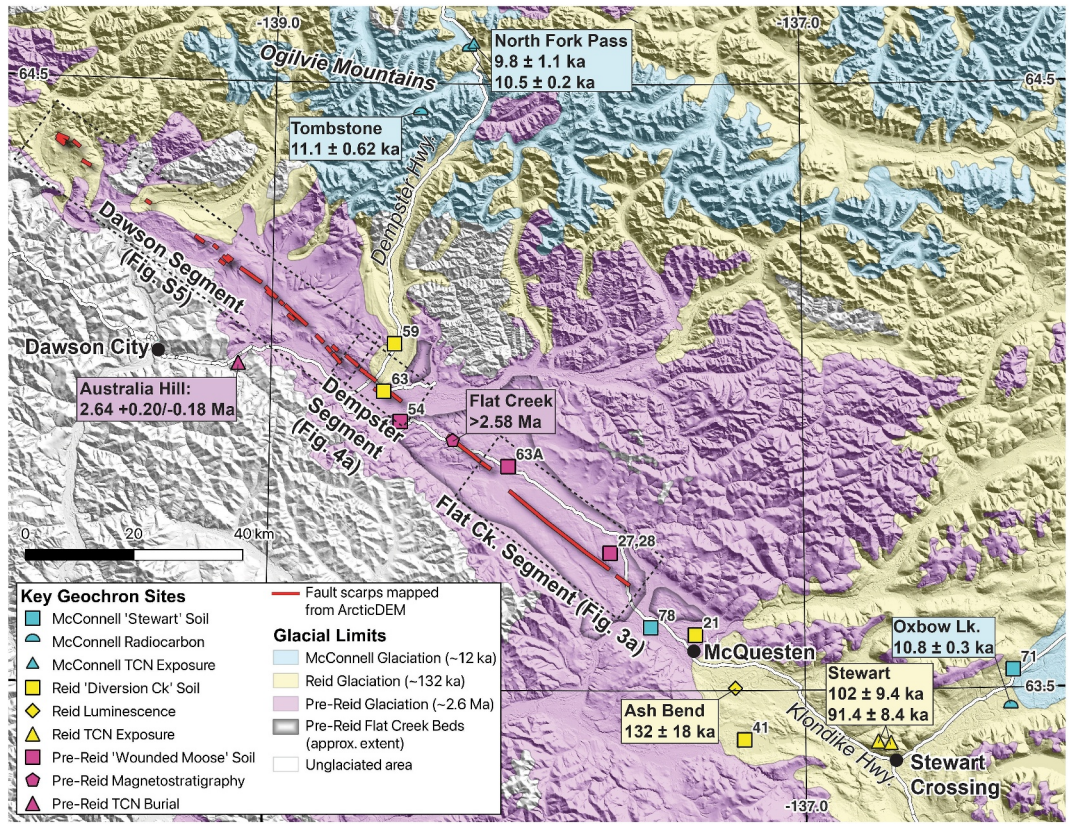

Figure 2. Map of Quaternary fault scarps (130 km total length) along the Tintina Trench in the Klondike region. Limits of the McConnell, Reid, and Pre-Reid ice are from Duk-Rodkin (1999). Direct age constraints are shown in boxes (also see Table S1 in Supporting Information S1). Numbered squares correspond to characteristic soil weathering profiles in Figure S7 in Supporting Information S1. Some sample sites occur on glaciofluvial outwash terraces and are therefore beyond the ice limit of the corresponding glaciation. Basemap is ArcticDEM version 4 (Porter et al., 2023).

Using new ArcticDEM and drone lidar topographic data (Salomon et al., 2024), surficial mapping, and geochronological constraints (see Text S1 in Supporting Information S1), we provide the first conclusive evidence for large surface-rupturing earthquakes on the Tintina fault in the Quaternary (2.6 Ma to present). We further show that despite rupturing numerous times throughout the Pleistocene (2.6 Ma to ~12 ka), the Tintina fault has not ruptured in a large event in the Holocene (12 ka to present) and may be late in its seismic cycle, which has significant seismic hazard implications. Our findings highlight a pitfall of relying on the short Holocene paleoseismic record for seismic hazard analysis and show that in low-strain-rate regions, existing, mature faults can accommodate strain via large earthquakes with recurrence intervals on the order of $>10^4$ years.

2. Geomorphic Evidence of Pleistocene Surface Ruptures on the Tintina Fault

We map a series of semi-continuous lineations and scarps spanning 130 km along the Tintina Trench (Figure 2). The fault traces offset and deform glacial and proglacial sediments and surfaces of Reid (132 ka) and Pre-Reid (2.6 Ma) ages. Below, we describe three distinct segments of the fault, here named the Flat Creek, Dempster, and Dawson segments.

2.1. The Flat Creek Fault Segment

The 52-km-long Flat Creek fault segment crosses a broad plain southwest of the Klondike Highway (Figure 3). Here, 2.6 Ma Pre-Reid outwash gravels and till (Froese et al., 2000) are deformed by an up to 20-m-high scarp and a series of en-echelon mounds and depressions that we interpret as positive and negative flower structures. A shallow test pit on one of the mounds (blue star; Figure 3) confirms a composition of clast-supported pebble-cobble gravel, weathering to reddish brown, consistent with Pre-Reid glaciofluvial deposits (Smith

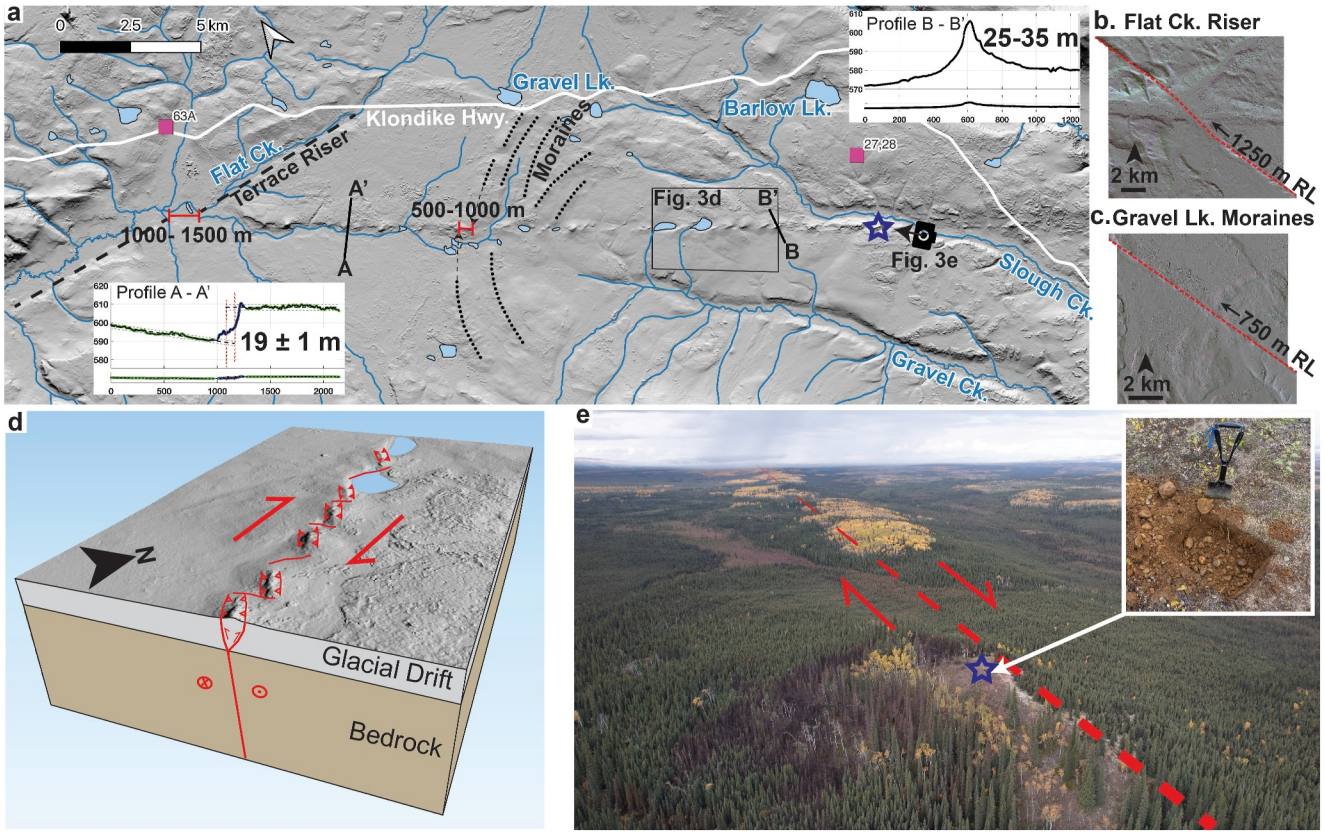

Figure 3. Detailed view of the Flat Creek fault segment. (a) ArcticDEM (Porter et al., 2023) hillshade showing the scarp cross-cutting the 2.6 Ma Flat Creek Beds. See Figure 2 for map extent. Topographic profiles are shown with both 1:1 scale (lower) and a vertical exaggeration (upper). (b, c) Median back-slip restorations (from LaDiCaoz) of 1,250 m right lateral offset to Flat Creek riser and 750 m right lateral offset to Gravel Lk. moraines. (d) 3D model and kinematic interpretation of the en-echelon push-ups. (e) Drone photo looking northwest along fault trace showing dense boreal forest cover. Push-up structures are highlighted by groves of yellow birch trees. Inset image shows subrounded cobble gravel and reddish-brown soil characteristic of Pre-Reid "Wounded Moose" paleosol in test pit located at blue star at top of push-up.

et al., 1986; Tarnocai et al., 1985). The pull-apart depressions are commonly occupied by sag ponds. The push-up structures are on the order of 300 m long, 50 m wide, and 20–40 m high, at least an order of magnitude larger than coseismic "mole tracks" observed along continental strike-slip surface ruptures (Choi et al., 2018; Little et al., 2021; Rizza et al., 2015). However, they closely resemble larger push-up structures and pressure ridges observed along the Kunlun fault in northern Tibet (Fu et al., 2003; Lin et al., 2004), and the Denali fault in southwestern Yukon (Blais-Stevens et al., 2020; Finley et al., 2022; Haeussler et al., 2017), which are interpreted to record cumulative mole-track-style deformation resulting from transpression. Tibet and the Yukon both have semi-continuous permafrost at present, and such surface deformation may be a consequence of the rheological properties of frozen ground in thick surficial sediments. In addition to the push-up structures being indicative of dextral transpression, we interpret a set of subdued, arcuate, northwestward-convex ridges as Pre-Reid terminal moraines; these are dextrally offset by 500–1,000 m (Figure 3 and Figure S1 in Supporting Information S1). The Flat Creek valley riser appears dextrally offset by 1,000–1,500 m, though this may exceed the true tectonic offset due to erosion of the riser by the creek immediately north of the fault.

2.2. The Dempster Fault Segment

The 7.7-km-long Dempster fault segment crosses the Dempster Highway northeast of the Klondike Highway junction. A fault scarp offsets terraces of Reid age (Gt-R), but does not deform terraces of McConnell age (Gt-M), nor the modern floodplain of the Klondike and North Klondike Rivers (Figure 4 and Figure S2 in Supporting Information S1). The scarp has a consistently northeast-side-up vertical separation of 3.3 ± 2.5 m (Figure S4 in Supporting Information S1). A discontinuous terrace riser, interpreted as late-Reid because it merges with a Reid-

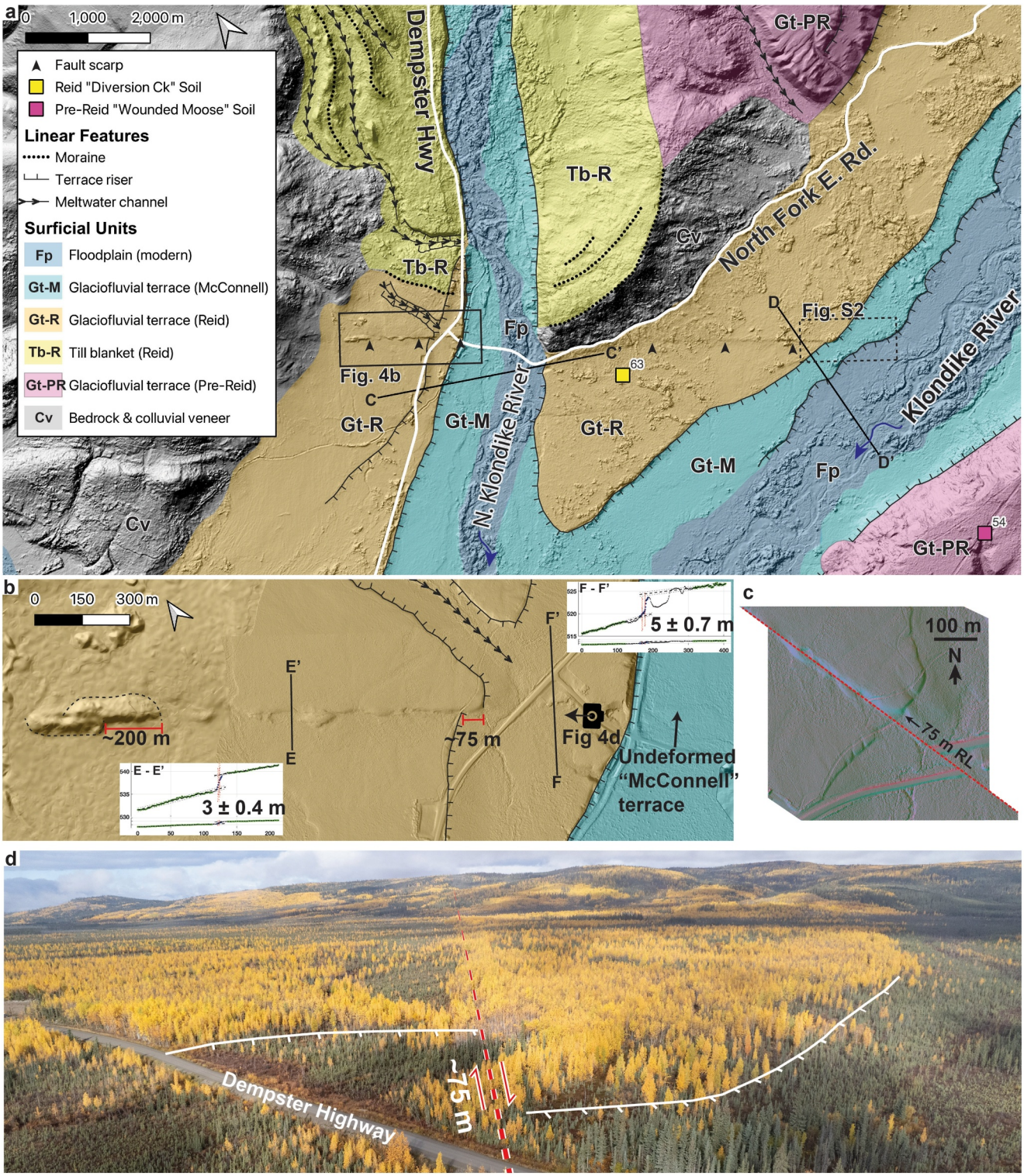

Figure 4. Detailed view of the Dempster fault segment. (a) Surficial map of the Dempster fault segment, based on existing maps (Duk-Rodkin, 1996; Froese, 2005a, 2005b; McKenna & Lipovsky, 2014; Thomas & Rampton, 1982) and augmented with new high-resolution topography. See Figure 2 for map extent. Topographic profiles C-C′ and D-D′ are provided in Figure S3 in Supporting Information S1. (b) Detailed map of the Dempster fault segment. Base map is drone lidar data. The ~132 ka Reid-age terrace surface is vertically offset by 3.3 ± 2.5 m, and dextrally offset by 65–85 m. Topographic profiles are shown with both 1:1 scale (lower) and a vertical exaggeration (upper). (c) LaDiCaoz restoration of median 75 m right lateral offset of terrace riser. (d) Drone photo looking northwest along fault trace, with annotation showing dextrally offset riser.

age outwash channel (rather than incising it), is dextrally offset by 65–85 m (Figure 4). This riser may have been trimmed or reworked, but this would have occurred primarily on the upstream side of the fault making our offset measurement an underestimate. We consider this riser the most reliable offset marker available and use it as a primary constraint on slip rate. Two less clearly defined features with apparent dextral offsets of ∼200 and ∼130 m (Figure 4 and Figure S2 in Supporting Information S1) provide supporting evidence, but we consider them less reliable for slip rate calculation (see Text S1 in Supporting Information S1 for details).

2.3. The Dawson Fault Segment

The Dawson segment extends for a further 70 km northwest, passing within 20 km of Dawson City (Figure 2 and Figure S5 in Supporting Information S1). This fault segment has more topographic relief than the Flat Creek and Dempster segments; colluvial and mass wasting processes are more dominant, contributing to poorer scarp preservation. We map a series of discontinuous lineaments and scarps, most of which exhibit northeast-side-up separation with no evidence of lateral offset. These scarps deform surfaces mapped as glaciofluvial terraces, till plains, and till veneers of both Reid and Pre-Reid age (Duk-Rodkin, 1996). We attribute the lack of observable lateral offset to the fact that channel offsets are poorly preserved on low-slip-rate faults over long time periods, as the channels tend to avulse to straighter paths (Dascher-Cousineau et al., 2021; Reitman et al., 2022). Cumulative lateral offsets are better preserved by static geomorphic features on flat terrain, such as the terrace risers and moraines on the Flat Creek and Dempster segments. Thus, we are confident in our interpretation of predominantly strike-slip kinematics on the Tintina fault despite the preservational bias towards the relatively minor dip-slip component.

3. Analyses and Implications

3.1. A Low Slip Rate and a Long, Open Interseismic Interval

Our measurements of deformed and undeformed Quaternary landforms indicate that the modern kinematics of the Tintina fault are dominantly right-lateral and the slip rate is low. The lack of deformation on McConnell-age terraces suggests that there has been no surface rupture or aseismic slip at least since the McConnell ice sheet receded from the Ogilvie Mountains ≥12 ka (Dalton et al., 2023; Menounos et al., 2017; Stroeven et al., 2010). Thus, if the total 65–85 m of right-lateral offset of the Reid-aged terrace riser occurred between the ends of the Reid and McConnell glaciations, we estimate a closed-interval slip rate of 0.5–0.8 mm/yr (Figure 5). This rate is consistent within uncertainty both with a longer-term closed-interval slip rate of 0.2–0.6 mm/yr that can be estimated from the 500–1,500 m right-lateral offsets to the Pre-Reid (ca. 2.6 Ma) Flat Creek beds (Figure 5), and with a slip rate estimate of 0.5 (+0.9/−0.3) mm/yr from seismic moment summation (Leonard et al., 2008). Given that regional GNSS velocities indicate northeastward convergence (Figure 1), there may be some degree of strain partitioning between strike-slip along the Tintina fault and active shortening across thrust belts to the northeast (Leonard et al., 2008).

We suggest that the lack of surface rupture through McConnell-aged and younger deposits is due to a currently open interseismic interval of at least 12 kyr, rather than waning tectonic activity. It is impossible from surface morphology alone to determine the frequency of earthquakes preserved in the landscape. Low-slip-rate faults are known to have long and variable intervals between earthquakes with differing average slip per event (Griffin et al., 2020; Nicol et al., 2016; Yuan et al., 2018), though this behavior may be moderated by the high structural maturity of the Tintina fault (Berryman et al., 2012; Thakur & Huang, 2021). However, most large strike-slip ruptures globally have <10 m slip (Wesnousky, 2008), so we can infer that the 65–85 m of lateral offset on the Dempster fault segment likely records at least ∼7 major earthquakes. The 500–1,500 m dextral offsets on the Flat Creek segment potentially record >100 individual earthquakes throughout the entire Quaternary Period. These measurements therefore provide robust long-term slip rates that average out any temporal variations (Styron, 2019). Further paleoseismic investigations are required to determine the recurrence intervals between past earthquakes, and whether slip rates have changed through time due to shifts in tectonic regime, or glacial isostatic adjustment.

3.2. Potential for Large Earthquakes

Using empirical scaling relations between maximum surface slip, surface rupture length, and moment magnitude (Wesnousky, 2008) we find that the Tintina fault is capable of large earthquakes despite its low slip rate. The

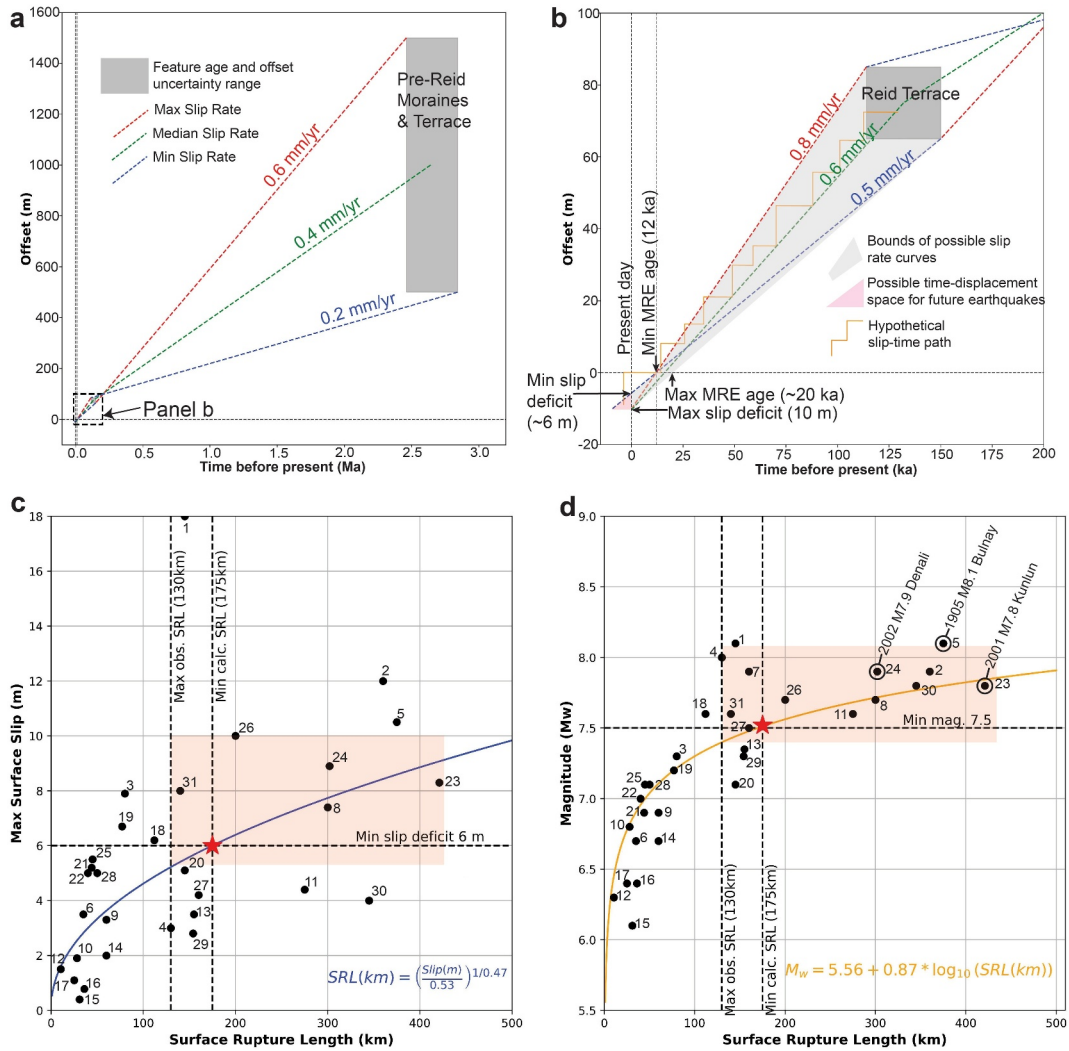

Figure 5. Slip rate and magnitude calculations. (a, b) Range of closed-interval slip rates calculated from offsets to Pre-Reid-age moraines and terraces, Reid-age terrace riser, and the inferred most recent event (MRE) >12 ka (see Text S1 in Supporting Information S1). Slip deficits are projected into the open interval to define range of possible time-displacement positions for future earthquakes. (c) Empirical power-law scaling relation between maximum surface slip and surface rupture length (Wesnousky, 2008). A minimum slip deficit of 6 m corresponds to a surface rupture length of 175 km (red star). (d) Empirical scaling relation between surface rupture length and M_w (Wesnousky, 2008). A 175 km surface rupture length corresponds to a minimum moment magnitude of 7.5 (red star). (c, d) Include datapoints from historical, instrumentally recorded strike-slip earthquakes (indexed in Table S2 in Supporting Information S1). The orange rectangles indicate full range of plausible values.

~130 km length of visible surface rupture corresponds to M_w 7.4 (Figure 5), but we view both the rupture length and associated magnitude as underestimates given the inferred long open interval and consequent likelihood that parts of the scarp have been substantially eroded, particularly in sloped terrain. Taking the 12 kyr minimum recurrence interval and the 0.5 mm/yr late Quaternary minimum slip rate, the fault will have accumulated at least 6 m of slip deficit since it last ruptured (Figure 5), a value within the range of modern strike-slip surface ruptures (Wesnousky, 2008). Coseismic slip of 6 m empirically predicts a rupture length of 175 km and M_w 7.5 (Figure 5). The highly linear Tintina fault trace is likely conducive to long surface ruptures, with minimal steps and bends to arrest slip propagation (Wesnousky, 2006). Critically, our estimate of M_w 7.5 is a minimum, as the coseismic slip and corresponding rupture length could be larger (and the recurrence interval longer). The resemblance of the Tintina scarp morphology—particularly on the Flat Creek segment—to push-up structures along major faults in

Central Asia that have hosted $M_w > 7.8$ ruptures (Choi et al., 2018; Fu et al., 2003; Lin et al., 2004; Rizza et al., 2015) further supports the notion that the Tintina fault may be capable of similarly large earthquakes.

The fate of a potential ~175-km-long surface rupture beyond the 130-km-long scarp currently preserved is not known, but we note that Reid-age terraces directly along strike to the southeast near Stewart Crossing (Figure 2) are not visibly faulted. Surface ruptures may have extended northwestward into Alaska where the more mountainous terrain is less conducive to scarp preservation. A rupture extending to the northwest raises the possibility of a link with the active Preacher-Medicine Lake segment of the Tintina fault, near the hamlet of Central, Alaska (Figure 1 and Figure S6 in Supporting Information S1), ~210 km northwest of the termination of scarps we map in the Klondike region. This site exhibits a ~5-m-high north-side-up scarp that offsets a 18–12 ka surface of loess (Haeussler et al., 2024), though it lacks any clear lateral offsets.

3.3. Seismic Hazard Implications

Our results have significant implications for seismic hazard in the Yukon Territory and neighboring Alaska. If ≥12 kyr have elapsed since the last major earthquake, the fault may be at an advanced stage of strain accumulation. Notably, viscoelastic models show that geodetically derived strain rates will appear low across faults near the end of long recurrence intervals, with most of the strain having accumulated early in the seismic cycle (Wang et al., 2021). This modeling result is consistent with the fact that strain accumulation on the Tintina fault is currently unresolvable with GNSS (Elliott & Freymueller, 2020; Leonard et al., 2007). An $M_w \geq 7.5$ earthquake would cause severe shaking in Dawson City (population ~1,600), <20 km from the mapped fault trace (Figure 2), and could also damage important highways and nearby mines. Compounding the shaking hazard, the Klondike region is prone to landslides, which could be seismically triggered. In particular, the Moosehide Slide immediately north of Dawson City, and the newly discovered Sunnydale landslide directly across the Yukon River, both show ongoing signs of instability (Bodtker et al., 2023; Brideau et al., 2007). More work is needed to determine the impact of revising seismic hazard models to include the Tintina fault as a discrete fault source; due to its low slip rate and long recurrence time, changes to computed hazard values may only be marginal. However, the fact that it is late in an open interval highlights the importance of time-dependent seismic hazard models (Petersen et al., 2007) and the need for more paleoseismic data.

Owing to its position outside the limits of Late Pleistocene glaciation, the segments of the Tintina fault examined herein likely represent the longest tectono-geomorphic record of active faulting in Canada, and among the longest globally. Had this area been glaciated in the Late Pleistocene, no record of surface rupture would be preserved, and instrumental networks would provide little indication of the earthquake potential. Our results therefore suggest that the paucity of fault surface ruptures observed in other low-strain-rate regions of the Canadian Cordillera is due—at least in part—to a preservation problem arising from extensive Late Pleistocene glaciation (Figure 1) rather than a true absence of paleoseismic activity. These findings should motivate future paleoseismic studies of potentially active faults, particularly pre-existing mature structures that may localize strain in slowly deforming regions.

Conflict of Interest

The authors declare no conflicts of interest relevant to this study.

Data Availability Statement

ArcticDEM version 4 (Porter et al., 2023) is publicly available online under a Creative Commons CC4 license (https://www.pgc.umn.edu/data/arcticdem/). Our drone lidar data are hosted by Open Topography (Finley et al., 2024) under a Creative Commons CC BY-NC 4.0 license. The Government of Yukon lidar collection (Government of Yukon, 2025) is publicly available online at https://maps.mcelhanney.com/Vertisee/Yukon-GovLidar/. Our fault scarp traces are provided in text and ESRI shapefile format in the Zenodo data repository (Finley et al., 2025) under a Creative Commons CC4 license. All map figures were created with QGIS software, available for free under a GNU GPLv2+ license (QGIS.org, 2025). The Lateral Displacement Calculator (LaDiCaoz) was developed by Zielke and Arrowsmith (2012) and updated by Haddon et al. (2016), and is published on GitHub under a GNU GPL-3.0 license (https://github.com/OlafZielke-EQ/LaDiCaoz_v2). The

Monte Carlo Slip Statistics Tool (MCSST) was developed by Wolfe et al. (2020) and is published on GitHub under an MIT license (https://github.com/wolfefranklin/MCSST_2019).

Acknowledgments
This work occurred on the territory of the Tr'ondëk Hwëch'in and Na-Cho Nyäk Dun First Nations. We thank Jordan Ross and Hussain Malik of the Tr'ondëk Hwech'in Government for their support. Maurice Colpron, Panya Lipovsky, Kristen Kennedy, Derek Cronmiller, Magali Rizza, and Kristin Morell provided helpful input on this work. Paul Sanborn is thanked for providing XRD data for soil weathering profiles. Braeden Clark provided field assistance. T.F. was supported by an NSERC CGS-D scholarship, a Margaret Perkins Hess Graduate Fellowship from the University of Victoria, and a Geoffrey Bradshaw Memorial Scholarship from the Yukon Foundation. Research funding came from NSERC Discovery Grants awarded to E.N. and J.C., a Canada Research Chair to E.N., and a Polar Knowledge Canada Northern Scientific Training Program grant to T.F. Our lidar drone was funded by the Canada Foundation for Innovation and BC Knowledge Development Fund. Nadine Reitman and an anonymous reviewer provided helpful reviews.

References

Adams, J., Allen, T., Halchuk, S., & Kolaj, M. (2019). Canada's 6th generation seismic hazard model, as prepared for the 2020 National Building Code of Canada. In *Proceedings 17th World Conference on Earthquake Engineering* (p. 8). The Canadian Association for Earthquake Engineering.

Anderson, J. G., Biasi, G. P., & Wesnousky, S. G. (2017). Fault-scaling relationships depend on the average fault-slip rate. *Bulletin of the Seismological Society of America*, *107*(6), 2561–2577. https://doi.org/10.1785/0120160361

Berryman, K. R., Cochran, U. A., Clark, K. J., Biasi, G. P., Langridge, R. M., & Villamor, P. (2012). Major earthquakes occur regularly on an isolated plate boundary fault. *Science*, *336*(6089), 1690–1693. https://doi.org/10.1126/science.1218959

Blais-Stevens, A., Clague, J. J., Brahney, J., Lipovsky, P., Haeussler, P. J., & Menounos, B. (2020). Evidence for large Holocene earthquakes along the Denali Fault in southwest Yukon, Canada. *Environmental and Engineering Geoscience*, *26*(2), 149–166. https://doi.org/10.2113/EEG-2263

Bodtker, J., Cronmiller, D. C., Bond, J. D., & Shugar, D. (2023). The Sunnydale landslide, current understanding and research, Dawson (NTS 116B/3). In K. MacFarlane (Ed.), *Yukon Exploration and Geology 2022* (pp. 19–33). Yukon Geological Survey.

Bollinger, L., Klinger, Y., Forman, S. L., Chimed, O., Bayasgalan, A., Munkhuu, U., et al. (2021). 25,000 Years long seismic cycle in a slow deforming continental region of Mongolia. *Scientific Reports*, *11*(1), 17855. https://doi.org/10.1038/s41598-021-97167-w

Brideau, M.-A., Stead, D., Roots, C., & Orwin, J. (2007). Geomorphology and engineering geology of a landslide in ultramafic rocks, Dawson City, Yukon. *Engineering Geology*, *89*(3), 171–194. https://doi.org/10.1016/j.enggeo.2006.10.004

Choi, J.-H., Klinger, Y., Ferry, M., Ritz, J.-F., Kurtz, R., Rizza, M., et al. (2018). Geologic inheritance and earthquake rupture processes: The 1905 M ≥ 8 Tsetserleg-Bulnay strike-slip earthquake sequence, Mongolia. *Journal of Geophysical Research: Solid Earth*, *123*(2), 1925–1953. https://doi.org/10.1002/2017JB013962

Dalton, A. S., Dulfer, H. E., Margold, M., Heyman, J., Clague, J. J., Froese, D. G., et al. (2023). Deglaciation of the North American ice sheet complex in calendar years based on a comprehensive database of chronological data: NADI-1. *Quaternary Science Reviews*, *321*. 108345. https://doi.org/10.1016/j.quascirev.2023.108345

Dascher-Cousineau, K., Finnegan, N. J., & Brodsky, E. E. (2021). The life span of fault-crossing channels. *Science*, *373*(6551), 204–207. https://doi.org/10.1126/science.abf2320

Demuro, M., Froese, D. G., Arnold, L. J., & Roberts, R. G. (2012). Single-grain OSL dating of glaciofluvial quartz constrains Reid glaciation in NW Canada to MIS 6. *Quaternary Research*, *77*(2), 305–316. https://doi.org/10.1016/j.yqres.2011.11.009

Drooff, C., & Freymueller, J. T. (2023). New insights into the active tectonics of the northern Canadian Cordillera from an enhanced earthquake catalog. *Journal of Geophysical Research: Solid Earth*, *128*(12), e2023JB026793. https://doi.org/10.1029/2023JB026793

Duk-Rodkin, A. (1996). *Surficial geology, Dawson, Yukon Territory*. Geological Survey of Canada. *Open File 3288*.

Duk-Rodkin, A. (1999). *Glacial limits map of Yukon*. Indian & Northern Affairs Canada/Department of Indian & Northern Development: Exploration & Geological Services Division. Retrieved from https://data.geology.gov.yk.ca/Reference/42050#InfoTab

Duk-Rodkin, A., Barendregt, R. W., White, J. M., & Singhroy, V. H. (2001). Geologic evolution of the Yukon River: Implications for placer gold. *Quaternary International*, *82*(1), 5–31. https://doi.org/10.1016/S1040-6182(01)00006-4

Elliott, J., & Freymueller, J. T. (2020). A block model of present-day kinematics of Alaska and Western Canada. *Journal of Geophysical Research: Solid Earth*, *125*(7), 30. https://doi.org/10.1029/2019JB018378

Finley, T., Nissen, E., Cassidy, J., Salomon, G., & Stephen, R. (2024). Drone lidar surveys of the Tintina fault, Yukon, Canada, September 2023 [Dataset]. *OpenTopography*. https://doi.org/10.5069/G9MG7MR9

Finley, T., Nissen, E., Cassidy, J., Salomon, G. W., Leonard, L., & Froese, D. (2025). Line traces of Quaternary fault scarps along the Tintina fault, Yukon, Canada [Dataset]. *Zenodo*. https://doi.org/10.5281/zenodo.15392522

Finley, T., Salomon, G., Nissen, E., Stephen, R., Cassidy, J., & Menounos, B. (2022). Preliminary results and structural interpretations from drone lidar surveys over the Eastern Denali fault, Yukon. In K. MacFarlane (Ed.), *Yukon Exploration and Geology 2021* (pp. 83–105). Yukon Geological Survey.

Froese, D. G. (2005a). *Surficial geology, Flat Creek, Yukon Territory*. Geological Survey of Canada. *Open File 4592*.

Froese, D. G. (2005b). *Surficial geology, Medrick Creek, Yukon Territory*. Geological Survey of Canada. *Open File 4593*.

Froese, D. G., Barendregt, R. W., Enkin, R. J., & Baker, J. (2000). Paleomagnetic evidence for multiple Late Pliocene—Early Pleistocene glaciations in the Klondike area, Yukon Territory. *Canadian Journal of Earth Sciences*, *37*(6), 863–877. https://doi.org/10.1139/e00-014

Fu, B., Awata, Y., Kano, K., Lin, A., & Tsukuda, E. (2003). Coseismic surface deformation and engineering damage associated with the large strike-slip faulting: Lessons from the 2001 Mw 7.8 Central Kunlun earthquake. In *Annual report on active fault and Paleoearthquake researches* (Vol. 3, pp. 191–209).

Gabrielse, H., Murphy, D. C., & Mortensen, J. K. (2006). Cretaceous and Cenozoic dextral orogen-parallel displacements, magmatism, and paleogeography, north-central Canadian Cordillera. In J. W. Haggart, R. J. Enkin, & J. W. H. Monger (Eds.), *Paleogeography of the North American Cordillera: Evidence for and against large-scale displacements* (pp. 255–276). Geological Association of Canada Special Paper 46.

Government of Yukon. (2025). Government of Yukon Lidar Collection [Dataset]. Retrieved from https://maps.mcelhanney.com/Vertisee/YukonGovLidar/

Griffin, J. D., Stirling, M. W., & Wang, T. (2020). Periodicity and clustering in the long-term earthquake record. *Geophysical Research Letters*, *47*(22), e2020GL089272. https://doi.org/10.1029/2020GL089272

Haddon, E. K., Amos, C. B., Zielke, O., Jayko, A. S., & Bürgmann, R. (2016). Surface slip during large Owens Valley earthquakes. *Geochemistry, Geophysics, Geosystems*, *17*(6), 2239–2269. https://doi.org/10.1002/2015GC006033

Haeussler, P. J., Bender, A. M., Powers, P. M., Koehler, R. D., & Brothers, D. S. (2024). Updating the crustal fault model for the 2023 National Seismic Hazard Model for Alaska. In N. Ruppert, M. Jadamec, & J. Freymueller (Eds.), *Tectonics and seismicity of Alaska and Western Canada: Earthscope and beyond*. Wiley.

Haeussler, P. J., Matmon, A., Schwartz, D. P., & Seitz, G. G. (2017). Neotectonics of interior Alaska and the late Quaternary slip rate along the Denali fault system. *Geosphere*, *13*(5), 1445–1463. https://doi.org/10.1130/GES01447.1

Hidy, A. J., Gosse, J. C., Froese, D. G., Bond, J. D., & Rood, D. H. (2013). A latest Pliocene age for the earliest and most extensive Cordilleran Ice Sheet in northwestern Canada. *Quaternary Science Reviews*, *61*, 77–84. https://doi.org/10.1016/j.quascirev.2012.11.009

Kolaj, M., Halchuk, S., & Adams, J. (2023). *Sixth generation seismic hazard model of Canada: Final input files used to generate the 2020 National Building Code of Canada seismic hazard values*. Geological Survey of Canada. *Open File 8924*.

Leonard, L. J., Hyndman, R. D., Mazzotti, S., Nykolaishen, L., Schmidt, M., & Hippchen, S. (2007). Current deformation in the northern Canadian Cordillera inferred from GPS measurements. *Journal of Geophysical Research*, *112*(11), 1–15. https://doi.org/10.1029/2007JB005061

Leonard, L. J., Mazzotti, S., & Hyndman, R. D. (2008). Deformation rates estimated from earthquakes in the northern Cordillera of Canada and eastern Alaska. *Journal of Geophysical Research*, *113*(8), 1–18. https://doi.org/10.1029/2007JB005456

Lin, A., Guo, J., & Fu, B. (2004). Co-seismic mole track structures produced by the 2001 Ms 8.1 Central Kunlun earthquake, China. *Journal of Structural Geology*, *26*(8), 1511–1519. https://doi.org/10.1016/j.jsg.2004.01.005

Little, T. A., Morris, P., Hill, M. P., Kearse, J., Van Dissen, R. J., Manousakis, J., et al. (2021). Coseismic deformation of the ground during large-slip strike-slip ruptures: Finite evolution of "mole tracks". *Geosphere*, *17*(4), 1170–1192. https://doi.org/10.1130/GES02336.1

Mazzotti, S., & Hyndman, R. D. (2002). Yakutat collision and strain transfer across the northern Canadian Cordillera. *Geology*, *30*(6), 495–498. https://doi.org/10.1130/0091-7613(2002)030<0495:YCASTA>2.0.CO;2

McKenna, K., & Lipovsky, P. (2014). *Surficial geology, Dawson Region, Yukon, Parts of NTS 115O/14 & 15 and 116B/1, 2, 3 & 4*. Yukon Geological Survey. *Open File 2014-12*.

Menounos, B., Goehring, B. M., Osborn, G., Margold, M., Ward, B., Bond, J., et al. (2017). Cordilleran Ice Sheet mass loss preceded climate reversals near the Pleistocene Termination. *Science*, *358*(6364), 781–784. https://doi.org/10.1126/science.aan3001

Mortensen, J., & Von Gaza, P. (1992). Application of Landsat TM thermal imagery to structural interpretations of the Tintina Trench in west-central Yukon. In *Yukon Geology* (Vol. 3, pp. 214–222). Exploration and Geological Services Division, Yukon, Indian and Northern Affairs Canada.

Natural Resources Canada. (2024). Canadian National Earthquake Database [Dataset]. Retrieved from https://www.earthquakescanada.nrcan.gc.ca/stndon/NEDB-BNDS/index-en.php

Nicol, A., Robinson, R., Van Dissen, R., & Harvison, A. (2016). Variability of recurrence interval and single-event slip for surface-rupturing earthquakes in New Zealand. *New Zealand Journal of Geology and Geophysics*, *59*(1), 97–116. https://doi.org/10.1080/00288306.2015.1127822

Petersen, M. D., Cao, T., Campbell, K. W., & Frankel, A. D. (2007). Time-independent and time-dependent seismic hazard assessment for the State of California: Uniform California earthquake rupture forecast model 1.0. *Seismological Research Letters*, *78*(1), 99–109. https://doi.org/10.1785/gssrl.78.1.99

Porter, C., Howat, I., Noh, M., Husby, E., Khuvis, S., Danish, E., et al. (2023). ArcticDEM, Version 4.1 [Dataset]. https://doi.org/10.7910/DVN/3VDC4W

QGIS.org. (2025). QGIS geographic information system [Software]. *QGIS Association*. Retrieved from http://www.qgis.org

Reitman, N. G., Klinger, Y., Briggs, R. W., & Gold, R. D. (2022). Climatic influence on the expression of strike-slip faulting. *Geology*, *51*(1), 18–22. https://doi.org/10.1130/g50393.1

Rizza, M., Ritz, J.-F., Prentice, C., Vassallo, R., Braucher, R., Larroque, C., et al. (2015). Earthquake geology of the Bulnay Fault (Mongolia). *Bulletin of the Seismological Society of America*, *105*(1), 72–93. https://doi.org/10.1785/0120140119

Ryan, J., Hayward, N., & Jackson, L. E., Jr. (2017). Landscape antiquity and Cenozoic drainage development of southern Yukon, through restoration modeling of the Tintina fault. *Canadian Journal of Earth Sciences*, *54*(10), 1085–1100. https://doi.org/10.1139/cjes-2017-0053

Salomon, G., Finley, T., Nissen, E., Stephen, R., & Menounos, B. (2024). Mapping fault geomorphology with drone-based lidar. *Seismica*, *3*(1). https://doi.org/10.26443/seismica.v3i1.1186

Smith, C., Tarnocai, C., & Hughes, O. (1986). Pedological investigations of Pleistocene glacial drift surfaces in the Central Yukon. *Géographie Physique et Quaternaire*, *40*(1), 29–37. https://doi.org/10.7202/032620ar

Stroeven, A. P., Fabel, D., Codilean, A. T., Kleman, J., Clague, J. J., Miguens-Rodriguez, M., & Xu, S. (2010). Investigating the glacial history of the northern sector of the Cordilleran Ice Sheet with cosmogenic ^{10}Be concentrations in quartz. *Quaternary Science Reviews*, *29*(25), 3630–3643. https://doi.org/10.1016/j.quascirev.2010.07.010

Styron, R. (2019). The impact of earthquake cycle variability on neotectonic and paleoseismic slip rate estimates. *Solid Earth*, *10*(1), 15–25. https://doi.org/10.5194/se-10-15-2019

Tarnocai, C., Smith, S., & Hughes, O. L. (1985). Soil development on Quaternary deposits of various ages in the central Yukon Territory. In *Current Research, Part A* (pp. 229–238). Geological Survey of Canada.

Thakur, P., & Huang, Y. (2021). Influence of fault zone maturity on fully dynamic earthquake cycles. *Geophysical Research Letters*, *48*(17), 1–11. https://doi.org/10.1029/2021GL094679

Thomas, R. D., & Rampton, V. N. (1982). *Surficial geology and geomorphology North Klondike River, Yukon Territory*. Geological Survey of Canada Preliminary Map 6-1982. https://doi.org/10.4095/119397

Wang, K., Zhu, Y., Nissen, E., & Shen, Z.-K. (2021). On the relevance of geodetic deformation rates to earthquake potential. *Geophysical Research Letters*, *48*(11), e2021GL093231. https://doi.org/10.1029/2021GL093231

Wesnousky, S. G. (2006). Predicting the endpoints of earthquake ruptures. *Nature*, *444*(7117), 358–360. https://doi.org/10.1038/nature05275

Wesnousky, S. G. (2008). Displacement and geometrical characteristics of earthquake surface ruptures: Issues and implications for seismic-hazard analysis and the process of earthquake rupture. *Bulletin of the Seismological Society of America*, *98*(4), 1609–1632. https://doi.org/10.1785/0120070111

Wolfe, F. D., Stahl, T. A., Villamor, P., & Lukovic, B. (2020). Short communication: A semiautomated method for bulk fault slip analysis from topographic scarp profiles. *Earth Surface Dynamics*, *8*(1), 211–219. https://doi.org/10.5194/esurf-8-211-2020

Yuan, Z., Liu-Zeng, J., Wang, W., Weldon, R. J., Oskin, M. E., Shao, Y., et al. (2018). A 6000-year-long paleoseismologic record of earthquakes along the Xorkoli section of the Altyn Tagh fault, China. *Earth and Planetary Science Letters*, *497*, 193–203. https://doi.org/10.1016/j.epsl.2018.06.008

Zielke, O., & Arrowsmith, J. R. (2012). LaDiCaoz and LiDARimager—MATLAB GUIs for LiDAR data handling and lateral displacement measurement. *Geosphere*, *8*(1), 206–221. https://doi.org/10.1130/GES00686.1

References From the Supporting Information

Akciz, S. O., Sançar, T., Kıray, H. N., Zabcı, C., Köküm, M., Balkaya, M., et al. (2024). Primary surface rupture and slip distribution associated with the M_w 7.6 06 February 2023 Elbistan earthquake, Turkey. In *Proceedings of the EGU General Assembly 2024*. Copernicus Meetings. https://doi.org/10.5194/egusphere-egu24-13350

Avouac, J.-P., Ayoub, F., Wei, S., Ampuero, J.-P., Meng, L., Leprince, S., et al. (2014). The 2013, M_w 7.7 Balochistan earthquake, energetic strike-slip reactivation of a thrust fault. *Earth and Planetary Science Letters*, *391*, 128–134. https://doi.org/10.1016/j.epsl.2014.01.036

Beierle, B. D. (2002). Late Quaternary glaciation in the northern Ogilvie Mountains: Revised correlations and implications for the stratigraphic record. *Canadian Journal of Earth Sciences*, *39*(11), 1709–1717. https://doi.org/10.1139/e02-062

DuRoss, C. B., Gold, R. D., Dawson, T. E., Scharer, K. M., Kendrick, K. J., Akciz, S. O., et al. (2020). Surface displacement distributions for the July 2019 Ridgecrest, California, earthquake ruptures. *Bulletin of the Seismological Society of America*, *110*(4), 1400–1418. https://doi.org/10.1785/0120200058

Elliott, J. R., Nissen, E. K., England, P. C., Jackson, J. A., Lamb, S., Li, Z., et al. (2012). Slip in the 2010–2011 Canterbury earthquakes, New Zealand. *Journal of Geophysical Research*, *117*(B3). https://doi.org/10.1029/2011JB008868

Jaya, A., Nishikawa, O., & Jumadil, S. (2019). Distribution and morphology of the surface ruptures of the 2018 Donggala–Palu earthquake, Central Sulawesi, Indonesia. *Earth Planets and Space*, *71*(1), 144. https://doi.org/10.1186/s40623-019-1126-3

Klinger, Y., Etchebes, M., Tapponnier, P., & Narteau, C. (2011). Characteristic slip for five great earthquakes along the Fuyun fault in China. *Nature Geoscience*, *4*(6), 389–392. https://doi.org/10.1038/ngeo1158

Kozaci, O., Altunel, E., Koehler, R., Yildirim, C., & Clahan, K. (2024). M7.8 Kahramanmaras earthquake surface fault rupture and near-fault effect observations. *Japanese Geotechnical Society Special Publication*, *10*(11), 276–281. https://doi.org/10.3208/jgssp.v10.SS-6-03

Mackenzie, D., & Elliott, A. (2017). Untangling tectonic slip from the potentially misleading effects of landform geometry. *Geosphere*, *13*(4), 1310–1328. https://doi.org/10.1130/GES01386.1

Manighetti, I., Perrin, C., Gaudemer, Y., Dominguez, S., Stewart, N., Malavieille, J., & Garambois, S. (2020). Repeated giant earthquakes on the Wairarapa fault, New Zealand, revealed by Lidar-based paleoseismology. *Scientific Reports*, *10*(1), 2124. https://doi.org/10.1038/s41598-020-59229-3

Ren, J., Xu, X., Zhang, G., Wang, Q., Zhang, Z., Gai, H., & Kang, W. (2022). Coseismic surface ruptures, slip distribution, and 3D seismogenic fault for the 2021 M_w 7.3 Maduo earthquake, central Tibetan Plateau, and its tectonic implications. *Tectonophysics*, *827*, 229275. https://doi.org/10.1016/j.tecto.2022.229275

Rodgers, D. W., & Little, T. A. (2006). World's largest coseismic strike-slip offset: The 1855 rupture of the Wairarapa Fault, New Zealand, and implications for displacement/length scaling of continental earthquakes. *Journal of Geophysical Research*, *111*(B12). https://doi.org/10.1029/2005JB004065

Scharer, K. M., Salisbury, J. B., Arrowsmith, J. R., & Rockwell, T. K. (2014). Southern San Andreas fault evaluation field activity: Approaches to measuring small geomorphic offsets—Challenges and recommendations for active fault studies. *Seismological Research Letters*, *85*(1), 68–76. https://doi.org/10.1785/0220130108

Ward, B. C., Bond, J. D., Froese, D., & Jensen, B. (2008). Old Crow tephra (140 ± 10 ka) constrains penultimate Reid glaciation in central Yukon Territory. *Quaternary Science Reviews*, *27*(19), 1909–1915. https://doi.org/10.1016/j.quascirev.2008.07.012